Changing Seascapes, Stochastic Connectivity, and Marine Metapopulation Dynamics

James R. Watson,[1,*] Bruce E. Kendall,[2] David A. Siegel,[3] and Satoshi Mitarai[4]

1. Atmospheric and Oceanic Sciences Program, Princeton University, Princeton, New Jersey 08540; 2. Bren School of Environmental Science and Management, University of California, Santa Barbara, California 93106; 3. Department of Geography, University of California, Santa Barbara, California 93106; 4. Marine Biophysics Unit, Okinawa Institute of Science and Technology, 1919-1 Tancha Onna-son, Okinawa 904-0412, Japan

Submitted September 30, 2011; Accepted February 29, 2012; Electronically published May 24, 2012

Online enhancement: appendix.

abstract: The probability of dispersal from one habitat patch to another is a key quantity in our efforts to understand and predict the dynamics of natural populations. Unfortunately, an often overlooked property of this potential connectivity is that it may change with time. In the marine realm, transient landscape features, such as mesoscale eddies and alongshore jets, produce potential connectivity that is highly variable in time. We assess the impact of this temporal variability by comparing simulations of nearshore metapopulation dynamics when potential connectivity is constant through time (i.e., when it is deterministic) and when it varies in time (i.e., when it is stochastic). We use mathematical analysis to reach general conclusions and realistic biophysical modeling to determine the actual magnitude of these changes for a specific system: nearshore marine species in the Southern California Bight. We find that in general the temporal variability of potential connectivity affects two important quantities: metapopulation growth rates when the species is rare and equilibrium abundances. Our biophysical models reveal that stochastic outcomes are almost always lower than their deterministic counterparts, sometimes by up to 40%. This has implications for how we use spatial information, such as connectivity, to manage nearshore (and other) systems.

Keywords: stochasticity, metapopulation dynamics, matrix modeling, connectivity, larval dispersal, fisheries management.

Introduction

Determining the number of individuals that move from one habitat patch to another is vital to our ability to predict the dynamics of natural populations (Tilman and Kareiva 1997; Hanski 1998). Across multiple habitat patches, this connectivity quantifies the redistribution of abundances over a landscape and is key to understanding how metapopulations persist over time (Hanski 1998; Hastings and Botsford 2006), how they respond to disturbances (Ovaskainen and Hanski 2003; Urban et al. 2009; Bodin and Saura 2010), and how invasive species might spread through them (With 2002; Blackwood et al. 2010). Hence, accurate determinations of connectivity are critical to our ability to govern and maintain ecological systems (Possingham et al. 2000; Lubchenco et al. 2003). However, regardless of its importance, connectivity remains poorly understood for many systems. This is especially true for one particular property of connectivity: its temporal variability.

Broadly speaking, connectivity comprises two quantities: (1) the number of individuals at a source patch A and (2) the per capita probability of dispersal from A to a given destination patch B, or potential connectivity (Watson et al. 2010). The first part is demographic in nature; whatever affects the number of individuals at the source will alter the number of dispersing individuals from it. Indeed, there has been considerable attention paid to how changes in subpopulation abundances affect metapopulation dynamics. For example, spatially correlated disturbances can temporarily synchronize subpopulation abundances, leading to decreases in metapopulation persistence (Day and Possingham 1995; Johst and Drechsler 2003; Elkin and Possingham 2008). Potential connectivity is different; given certain dispersal abilities, it is defined largely by the landscape over which a species travels. It too has received considerable attention, and several sophisticated methods exist for calculating potential connectivity in spatially complex landscapes, ranging from network and circuit theory (e.g., McRae et al. 2008; Treml et al. 2008; Urban et al. 2009) to advection/diffusion approaches (e.g., Okubo and Levin 1989; Largier 2003). However, most analyses of potential connectivity assume that landscape features are static, not changing over ecological timescales. This results in a deterministic view of potential connectivity, which may be appropriate in some systems but not

* Corresponding author; e-mail: jrwatson@princeton.edu.

Am. Nat. 2012. Vol. 180, pp. 99–112.
DOI: 10.1086/665992

for others since there are many environments whose landscape features are highly dynamic.

Perhaps the most obvious landscapes with dynamic features are those belonging to the marine realm. For example, nearshore marine species are sedentary as adults, remaining local to habitat patches such as kelp forests or coral reefs (Roughgarden et al. 1988). Long-distance dispersal is achieved by newly spawned larvae dispersing with ocean currents, traveling distances ranging from tens to hundreds of kilometers (Kinlan et al. 2005; Cowen et al. 2006; Siegel et al. 2008; Mitarai et al. 2009). As a result, nearshore marine species exist in systems of interconnected subpopulations (Botsford et al. 2003; Watson et al. 2011*a*, 2011*b*). These seascapes were once thought to be uniformly connected and well mixed over ecological timescales (i.e., the larval pool assumption; Vance 1973), but we now know that nearshore potential connectivity is spatially heterogeneous. Larval dispersal trajectories are strongly affected by oceanographic features, such as mesoscale eddies, alongshore jets, and squirts. These provide structure and often create barriers to dispersal (Cowen et al. 2006; Watson et al. 2010). Importantly, we also know that these seascape features are highly dynamic, being present 1 year/month/day and not the next (Mitarai et al. 2009).

Over the past decade, coupled biophysical models have been used to make realistic determinations of nearshore potential connectivity (e.g., Cowen et al. 2006; Mitarai et al. 2009). These determinations have revealed often spatially complex patterns of potential connectivity, yet the temporal dimension of connectivity has received relatively little attention (although see Berkley et al. 2010). Here, our goal is to address this knowledge gap and investigate the influence of temporal variability in connectivity on the demographics of nearshore marine metapopulations.

We first develop basic theory behind how time-varying potential connectivity, as a source of environmental stochasticity (Lande and Orzack 1988; Gravel et al. 2011), alters nearshore metapopulation dynamics relative to when it is assumed to be constant. This work adapts and extends the theory of stage-structured populations, where the effect of stochastic parameters on, for example, the number of individuals transitioning between age states is well known (Tuljapurkar and Orzack 1980; Caswell 2001). We then numerically quantify the magnitude of these changes for a specific example: nearshore marine species in the Southern California Bight (fig. 1*a*). We determine patterns of potential connectivity by simulating dispersing larvae, using a Lagrangian probability density function method (Mitarai et al. 2009). This approach captures the complex spatial and temporal properties of potential connectivity in the nearshore of the Southern California Bight (Watson et al. 2010). Potential connectivity for a broad range of

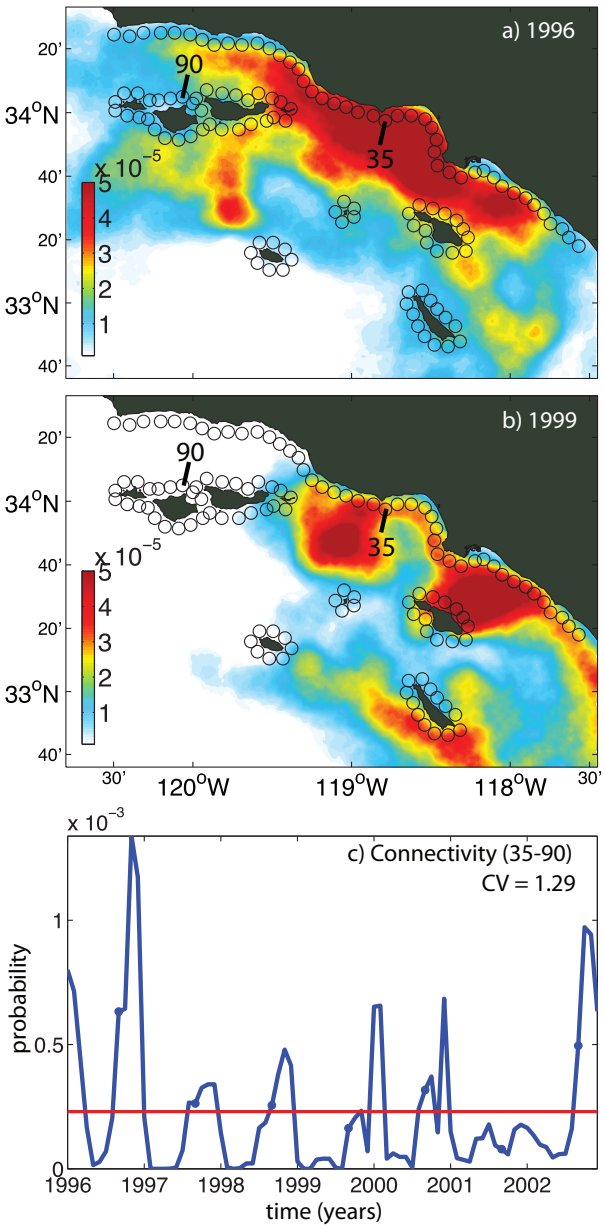

Figure 1: *a*, Example of a Lagrangian probability density function (PDF) for the Southern California Bight for Lagrangian particles released from patch 35 for the spawning period August–October, 1996, and a pelagic larval duration of 20 days. *b*, Same Lagrangian PDF but for 1999. Colors identify probability densities of Lagrangian particles (km^{-2}). Because ocean currents change annually, so do Lagrangian PDFs. Lagrangian PDFs are used to quantify the potential connectivity between a given pair of nearshore patches (circles). *c*, Associated potential connectivity time series (blue line; $D_{xy}(t)$) between patch 35 and patch 90; blue dots identify the mean August–October connectivity for each year, and the red line is the mean over the entire period (i.e., $\overline{D}_{35,90}$). The coefficient of variation (CV) for this time series is 1.29.

species is calculated over a 7-year period, and we also focus on two nearshore marine species with known dispersal characteristics: kelp bass *Paralabrax clathratus* and sheephead *Semicossyphus pulcher* (Love 1991; California Department of Fish and Game 2009). These determinations of potential connectivity are used to drive metapopulation models, with the aim of comparing deterministic and stochastic dynamics. For the purposes of this article, deterministic dynamics refer to when potential connectivity is constant through time (we address the scenario of deterministically time-varying potential connectivity in "Discussion"). We use the expectation in potential connectivity over the 7 years of data to develop deterministic dynamics. In contrast, stochastic dynamics refers to when potential connectivity varies in time. To create stochastic dynamics, we use the 7 years of potential connectivity data independently. We compare deterministic and stochastic outcomes using two fundamental metapopulation quantities: (1) metapopulation growth rates when a species is rare and (2) equilibrium abundances.

Metapopulation Model Analysis

Deterministic and stochastic nearshore metapopulation dynamics were compared using a simple single-species model:

$$n_x(t+1) = n_x(t)(1-m) + g(s_x(t)), \tag{1}$$

where $n_x(t+1)$ is the future number of adults at subpopulation x. The time step is 1 year, reflecting the annual reproductive cycle of many nearshore species. The first term quantifies adult survival, where m is the natural mortality, and the second term quantifies the number of new recruits to subpopulation x at time t. The number of recruits, $g(s_x(t))$, is a function of the number of larvae settling to x after their pelagic dispersal. This is typically a nonlinear function describing postsettlement density-dependent larval mortality, but here, to maintain generality, we leave this function unspecified. The number of settlers $s_x(t)$ is defined as

$$s_x(t) = \sum_y n_y(t) f D_{xy}(t), \tag{2}$$

where $D_{xy}(t)$ is the probability of a larva traveling from a spawning site y to a destination location x at time t. This is the potential connectivity (Watson et al. 2010, 2011*b*). The summation calculates the total number of settling larvae arriving from all spawning locations (y), and f is the per capita fecundity. Our model assumes that reproduction occurs before adult mortality.

Dynamics When a Species Is Rare

At low larval abundances, density dependence, either negative or positive, is assumed negligible. In its place, we assume that density-independent larval mortality occurs with $g(s_x) = \gamma s_x$, where γ is simply the fraction of larvae that survive settlement (Hastings and Botsford 2006). The population dynamics are now a simple linear function of $n_x(t)$. Adopting matrix notation, the dynamics are

$$\mathbf{n}(t+1) = \mathbf{C}(t)\mathbf{n}(t), \tag{3}$$

where $\mathbf{n}(t)$ is the vector of subpopulation abundances and $\mathbf{C}(t)$ is the metapopulation projection matrix, with elements

$$C_{xy}(t) = \begin{cases} (1-m) + \gamma f D_{xy}(t) & \text{if } x = y \\ \gamma f D_{xy}(t) & \text{if } x \neq y. \end{cases} \tag{4}$$

The elements $C_{xy}(t)$ are termed subpopulation connections because, in the case of self-connectivity ($x = y$), they account for both larval dispersal between subpopulations and adult survivability.

If potential connectivity were assumed to be constant through time, for example, if we considered the temporal expectation only, then the metapopulation projection matrix would also be constant (i.e., $\overline{\mathbf{C}}$). Quantifying whether the metapopulation persists is then simply a matter of finding the dominant eigenvalue of $\overline{\mathbf{C}}$, here termed λ_1. In contrast, if dispersal probabilities change with time, this simple calculation cannot be made. Instead, the total abundance of the metapopulation can be expressed as

$$\begin{aligned} \sum_x n_x(t) &= \| \mathbf{n}(t) \| \\ &= \| \mathbf{C}(t-1)\mathbf{C}(t-2) \ldots \mathbf{C}(0)\mathbf{n}(0) \| , \end{aligned} \tag{5}$$

where $\mathbf{n}(0)$ is a vector of initial subpopulation abundances and $\|.\|$ is the vector norm. For this system, there exists a number (λ_s) such that

$$\begin{aligned} &\lim_{t\to\infty} \frac{1}{t} \log \sum_x n_x(t) \\ &= \lim_{t\to\infty} \frac{1}{t} \log \| \mathbf{C}(t-1)\mathbf{C}(t-2) \ldots \mathbf{C}(0)\mathbf{n}(0) \| \\ &= \log \lambda_s. \end{aligned} \tag{6}$$

λ_s is the stochastic metapopulation growth rate, and it is a better estimate of the metapopulation growth rate than its deterministic counterpart (λ_1) because it takes into account the temporal variability of potential connectivity. λ_s can be found through numerically simulating the above formula or by Tuljapurkar's approximation (Tuljapurkar and Orzack 1980),

$$\log \lambda_s \approx \log \lambda_1 - \frac{1}{2}\left(\frac{\tau^2}{\lambda_1^2}\right), \tag{7}$$

with

$$\tau^2 = \sum_{xy}\sum_{kl} \mathrm{Cov}\,(C_{xy}, C_{kl}) Z_{xy} Z_{kl} = \sum_{xy} \tau_{xy}^2, \tag{8}$$

where for small deviations around the mean, τ^2 is a linear approximation to the variance in the deterministic growth rate (λ_1). $\mathrm{Cov}\,(C_{xy}, C_{kl})$ are the covariances between all possible pairs of subpopulation connections ($x, y, k, l =$ 1 ... the number of subpopulations), and Z_{xy} is the sensitivity of λ_1 to changes in a given subpopulation connection; formally, these sensitivities are defined as the partial derivative $\partial\lambda_1/\partial C_{xy}$. In our model, sensitivities are always positive, and as a result, we can see in equations (7) and (8) that positive covariances (i.e., synchronized connections) increase τ^2 and reduce λ_s relative to λ_1. The variance in self-connectivity, which includes variability in adult abundances (eq. [4]), is at all times positive and hence always reduces metapopulation growth rates when rare. Negative covariances between connections (i.e., asynchrony) are possible and, similar to positive covariances, arise from the underlying oceanography. For example, oceanographic features, such as alongshore jets, can connect multiple sites at the same time, resulting in positive covariances between multiple connections (Mitarai et al. 2009). Concurrently, these features can also disconnect sites, leading to negative covariances between connections.

Equations (5)–(8) are well understood for stage-structured populations (Tuljapurkar and Orzack 1980; Caswell 2001). However, in the metapopulation setting, the Tuljapurkar approximation provides new spatial information. For example, every subpopulation connection (C_{xy}) has a temporal covariance with all others (C_{kl}). Weighting these covariances by their sensitivities and then summing them for each connection defines τ_{xy}^2 (right-hand term in eq. [8]). These values identify the contribution of each connection to τ^2 and hence the change in metapopulation growth rate when rare. For example, positive (negative) τ_{xy}^2 values identify connections that, because of their sensitivities and covariances with other connections, reduce (increase) the metapopulation growth rate when rare.

Dynamics When Abundant

When abundances are high, larval density dependence cannot be ignored, and we revert to the original model (eq. [1]), using the function $g(s_x)$ to identify the number of settlers that recruit to an adult population.

Under most conditions, deterministic metapopulation dynamics eventually reach equilibrium (denoted by an asterisk), and the growth rate of each subpopulation becomes 0. At this point, the loss of adults due to natural mortality is balanced by the gain of new recruits:

$$n_x^* m = r_x^* = g(s_x^*), \tag{9}$$

where r_x^* is the number of larval recruits at subpopulation x at equilibrium. Hereafter, we assume equilibrium conditions and drop the asterisk for the sake of brevity. It is possible that certain deterministic functions of settlement ($g(s_x)$) could lead to cycles or chaos (e.g., if it is Ricker-like), but since natural mortality in nearshore populations is small and adult longevity is high, it requires extreme density dependence parameter values to achieve these dynamics.

Under stochastic conditions, the variables (n_x, s_x, r_x) continue to vary in time, eventually reaching stationary states. We compare stochastic stationary states with deterministic equilibriums by recasting equation (9) in terms of the expected number of larval recruits at a given subpopulation over time:

$$\mathrm{E}(r_x) = \mathrm{E}(g(s_x)). \tag{10}$$

Then, by a second-order Taylor expansion around the mean number of settlers, $\mathrm{E}(s_x)$, we obtain

$$\mathrm{E}(r_x) \approx \mathrm{E}\left(g(\mathrm{E}(s_x)) + g'(\mathrm{E}(s_x))[s_x - \mathrm{E}(s_x)] - \frac{g''(\mathrm{E}(s_x))}{2}[s_x - \mathrm{E}(s_x)]^2\right). \tag{11}$$

Here, many terms simplify, including the first-order term, which, because $\mathrm{E}(s_x - \mathrm{E}(s_x)) = 0$, vanishes entirely. Ultimately, the expected number of recruits is approximated as

$$\mathrm{E}(r_x) \approx g(\mathrm{E}(s_x)) - \frac{g''(\mathrm{E}(s_x))}{2}\mathrm{Var}\,(s_x), \tag{12}$$

and we see that, assuming that $g''(\mathrm{E}(s_x)) > 0$, the temporal variability in settlement ($\mathrm{Var}\,(s_x)$) reduces the expected number of recruits at a given subpopulation and hence subpopulation abundances (i.e., Jensen's inequality; Ruel and Ayres 1999). From the opposite perspective, if the settlement variance is 0, then the expectation of the stochastic stationary distribution is equal to the deterministic equilibrium.

Metapopulation Simulations

Potential Connectivity in the Southern California Bight

Dispersing larvae were simulated as passive Lagrangian particles within a regional ocean modeling system (ROMS) solution for the Southern California Bight (Dong et al. 2009; Mitarai et al. 2009). The ROMS solution has 40

vertical levels and a horizontal spatial resolution of 1 km, with all eight islands in the Southern California Bight resolved. The model captures the complex circulation of the Southern California Bight and shows strong correspondence with observed ocean conditions (Dong et al. 2009; Ohlmann and Mitarai 2010). Approximately 50 million passive Lagrangian particles were released over the period January 1, 1996–December 31, 2002, across 135 circular patches (5 km in radius) distributed uniformly throughout the nearshore (fig. 1*a*). Particles were released every 12 h and, as they advected with ocean currents, their location recorded every 15 min for 90 days or until they left the domain (for more details, see Mitarai et al. 2009).

Lagrangian probability density functions (PDFs) were then used to calculate the site-to-site transition probabilities that define potential connectivity (Mitarai et al. 2009). As an example, see figure 1*a* and 1*b* for Lagrangian PDFs from two different years; Lagrangian particles were released from a particular nearshore patch during the period August–October, 1996 (fig. 1*a*) and 1999 (fig. 1*b*), and then were allowed to advect with the ROMS velocities for 20 days. Their locations after this advection time define the Lagrangian PDF, and from this, the potential connectivity between a given nearshore source and destination patch is calculated (Mitarai et al. 2009). This was done for a subset of 117 pairs of patches for every spawning month triplet and year (*t*; January–December, 1996–2002) and for a range of advection times, or pelagic larval durations (1–90 days). The later two dispersal parameters identify different modeled species. The patch subset was chosen to minimize artificial demographic effects created by the domain edge (see fig. A1, available online), and the middle month is used to identify spawning month triplets (e.g., September refers to the connectivity of August, September, and October).

Assuming that nearshore marine species spawn once a year, over a given monthly triplet, a set of seven independent spawning years (1996–2002) was calculated for each species (for a potential connectivity time series, see fig. 1*c*). Thus, species-specific potential connectivity between all pairs of patches is a function of pelagic larval duration, spawning month, and year. The range of pelagic larval durations and spawning months allowed us to calculate potential connectivity for a broad range of modeled species, but we also focused our attention on two species with contrasting dispersal parameters: a species that spawns in the fall with a short pelagic larval duration (30 days) and a spring spawning species with a long pelagic larval duration (60 days). These parameter values represent two common species in the Southern California Bight: kelp bass *Paralabrax clathratus* and sheephead *Semicossyphus pulcher*, respectively (Roughgarden et al. 1988; California Department of Fish and Game 2009).

Metapopulation Simulations without Density Dependence

We numerically solved for deterministic and stochastic metapopulation growth rates when rare for every modeled species (i.e., for the potential connectivity associated with every combination of pelagic larval duration and spawning period). Using the linear model with no larval density dependence (eq. [3]), values of f were chosen such that the deterministic growth rate (λ_1) for each species was equal to 1, and then stochastic growth rates (λ_s) were calculated through simulation. Initially, subpopulation abundances were equal and summed to 1; then, stochastic dynamics were iterated forward in time by randomly selecting a yearly potential connectivity matrix (D_{xy}(1996 ... 2002)), until a stationary distribution was reached (Morris and Doak 2002). This typically took 2,000 iterations. The stochastic metapopulation growth rate when rare was then calculated using equation (6).

The spatial structure of τ^2—the quantity that changes the metapopulation growth rate when rare (see eq. [8])—was explored by first analyzing τ_{xy}^2 values. These identify the contribution of a given subpopulation connection to τ^2. In order to reveal the geographic relationships between τ_{xy}^2 values, we used a k-means clustering algorithm on the sensitivity-weighted variance/covariance matrix. The clustering algorithm identifies groups of connections on the basis of their weighted covariances with each other (eq. [8]), and it requires that the number of clusters be specified. We chose five clusters, since this separated the Southern California Bight into geographically meaningful groups. Last, we calculated $\sum_{\text{group}} \tau_{xy}^2$, which identifies whether a particular group of subpopulation connections increases or decreases τ^2 and the metapopulation growth rate when rare.

Metapopulation Simulations with Density Dependence

We also examined the effect of stochastic potential connectivity on equilibrium abundances, specifying the density dependence function:

$$g(s_x(t)) = \frac{\gamma s_x(t)}{1 + \beta s_x(t)}. \tag{13}$$

This Beverton-Holt functional form is commonly used to describe postsettlement density dependence, where, because of larvae-on-larvae competition, only a fraction of larvae survive to recruit to the adult population (Hilborn and Walters 1992). Here, γ is the density-independent parameter quantifying the fraction of larvae that survive settlement, and β is the parameter controlling the intensity of density dependence. With this function, we are able to specify the analytical approximation for the expected number of recruits at a given subpopulation (eq. [12]). First,

the second derivative of the expected number of larval settlers is

$$g''(\mathrm{E}(s_x)) = \frac{2\gamma\beta}{[1 + \beta\mathrm{E}(s_x)]^3}. \quad (14)$$

Then, using the Taylor expansion, the expected number of recruits is approximated as

$$\mathrm{E}(r_x) \approx \frac{\gamma\mathrm{E}(s_x)}{1 + \beta\mathrm{E}(s_x)}\left\{1 - \frac{\beta\,\mathrm{Var}\,(s_x)}{\mathrm{E}(s_x)[1 + \beta\mathrm{E}(s_x)]^2}\right\}. \quad (15)$$

Again, similar to the general case (eq. [12]), the temporal variance in larval settlement ($\mathrm{Var}\,(s_x)$) decreases recruitment and hence also equilibrium abundances. If it were 0, equation (15) would reduce to the deterministic case, equation (13).

Both the expectation and the variance in settlement—$\mathrm{E}(s_x)$ and $\mathrm{Var}\,(s_x)$, respectively—will be affected by the temporal statistics of adult abundances and potential connectivity. In order to understand which drives the changes in equilibrium abundances, we made a further approximation that assumed that adult abundances were constant over space (x) and time (t), or $\bar{n}$. Using the rules $\mathrm{E}(aX) = a\mathrm{E}(X)$, where a is a constant, and $\mathrm{Var}\,(X) = \mathrm{E}(X^2) - \mathrm{E}(X)^2$, we approximated the expectation and variance in settlement using the statistics of the potential connectivity alone:

$$\mathrm{E}(s_x) \approx \bar{n}f\,\mathrm{E}\left(\sum_y D_{xy}\right),$$

$$\mathrm{Var}\,(s_x) \approx \bar{n}^2 f^2\,\mathrm{Var}\left(\sum_y D_{xy}\right), \quad (16)$$

where expectations and variances are over time.

Numerical simulations of the density-dependent model were made using realistic parameters. We set γ equal to 1, m equal to 0.2, and the carrying capacity (K) equal to 100 (our results are insensitive to this value). Since increasing f increases the number of settlers per adult, it also increases the fraction of settlers that must be killed in the density-dependent recruitment phase in order to ensure that total recruitment matches adult mortality at equilibrium. Thus, we varied the fecundity ($f = 0.5, 2, 5$) to create different levels of density dependence, solving for β, the density dependence parameter, given the relationship $\beta = (1/K)[(\gamma/m) - (1/f)]$, which comes from a nonspatial version of our model. Density dependence was measured using the compensation ratio (Goodyear 1980), defined as the ratio of the per capita settler survival rate at very low densities to the per capita settler survival rates at the highest possible density of settlers. Fecundities were chosen to produce realistic compensation ratios, ranging from 2.5 to 6 (varying with pelagic larval duration and spawning season; Bode et al. 2006; California Department of Fish and Game 2009).

Dynamics when abundant were simulated as follows. Initially, for each species, deterministic metapopulation dynamics were iterated forward in time using the annual average potential connectivity ($\overline{D}_{xy}$) until subpopulation abundances reached equilibrium. Then, stochastic metapopulation dynamics were explored by substituting the average potential connectivity with randomly drawn annual potential connectivity matrices (D_{xy}(1996 ... 2002)). Stochastic dynamics were iterated forward in time until subpopulation abundances reached stationary distributions. This was identified by inspecting the variance in the mean of each subpopulation's trajectory as the model progressed. Stationarity was achieved when all subpopulation abundance means, calculated over a 75-year window, converged to particular values (i.e., as standard errors diminished). We then compared deterministic equilibrium abundances with expectations of the stochastic stationary distributions for both the whole metapopulation and each subpopulation.

Simulation Results

For every species, the coefficient of variation (CV) in time for each potential connection (D_{xy}) was calculated. Taking the mean CV over all x, y pairs then describes how much, in general, that species' potential connectivity varies with time. Mean CV values ranged from 0.9 to 1.7, with most values above 1 (fig. 2*a*). This highlights that the annual variability in potential connectivity typically exceeds its expectation (Siegel et al. 2008; Mitarai et al. 2009). Further, the mean CV varied with the spawning period and pelagic larval duration (fig. 2*a*). The greatest mean CV was found in spring spawning periods (April–June) and at high pelagic larval durations (>50 days). This spawning period coincides with the upwelling season in the Southern California Bight (Mitarai et al. 2009), revealing the dependence of potential connectivity's temporal dynamics on the underlying ocean circulation of the Southern California Bight. Another area of parameter space with high mean CV is at low pelagic larval durations across all spawning periods.

Across species, stochastic potential connectivity reduced metapopulation growth rates when rare relative to deterministic dynamics (fig. 2*b*). Values of λ_s, the stochastic growth rate, were 10%–30% lower than λ_1, the deterministic growth rate. The difference between λ_s and λ_1 varied with spawning period and pelagic larval duration, with the largest drop in growth rates occurring during the spring months (February–May) and at high pelagic larval durations (>50 days). This area corresponds with the spawning

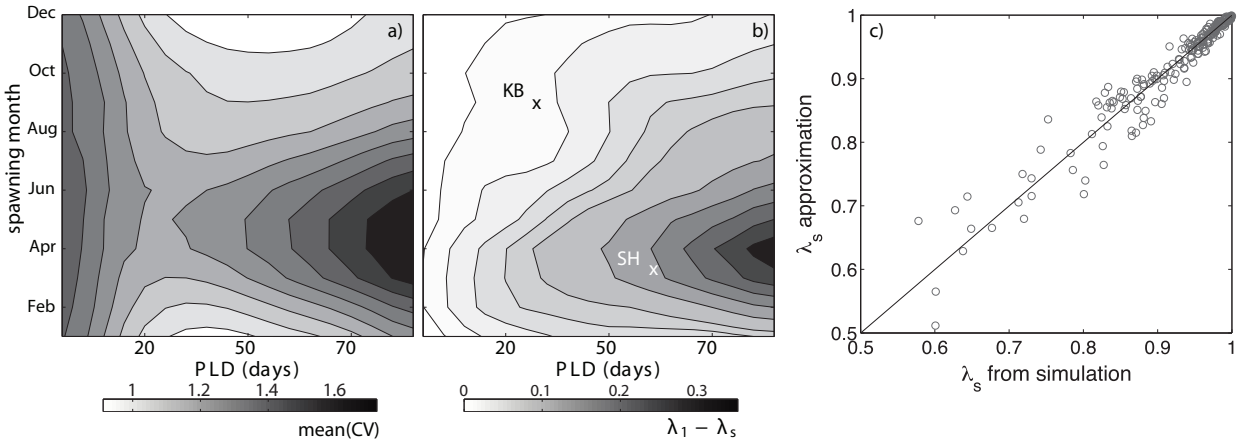

Figure 2: *a*, Mean across pairs of subpopulations of the coefficient of variation (CV) for the temporal variability in potential connectivity, for all combinations of pelagic larval duration (PLD; *X*-axis) and spawning month (*Y*-axis). *b*, Difference between deterministic (λ_1) and stochastic (λ_s) metapopulation growth rate when rare. The black and white crosses identify the pelagic larval duration and spawning months of kelp bass (KB) and sheephead (SH), respectively. *c*, Relationship between λ_s derived from simulation and through Tuljapurkar's approximation (eqq. [7], [8]; $R^2 = 0.92$).

periods and pelagic larval durations that have the greatest variability in potential connectivity (fig. 2*a*). Although species with low pelagic larval durations have large variability in potential connectivity, they did not show large changes in growth rates when rare, implying that these species have connections with low sensitivities (i.e., Z_{xy} in eq. [8]).

The Tuljapurkar approximation (eqq. [7], [8]) showed strong correspondence with simulation results (fig. 2*c*), even though it was designed for systems with small variance (Tuljapurkar and Orzack 1980). It is therefore a useful tool to further explore which features reduced metapopulation growth rates. We made a further approximation, where off-diagonal elements of the covariance/variance matrix were set to 0. This isolates the explanatory power of variance elements only and ignores the synchrony (i.e., positive covariances) between connections. This reduced Tuljapurkar approximation did not reproduce the simulated results or show any correspondence with the original approximation, which included covariance elements (see fig. A2, available online). This confirms that the temporal covariances between potential connections are key to the reduction in metapopulation growth rates when rare.

τ_{xy}^2 values identify the contribution of each subpopulation connection to the reduction in metapopulation growth rates when rare. The top 1% of τ_{xy}^2 for sheephead and kelpbass (137 connections in total) are plotted in figure 3*a* and 3*b*, respectively. Although only a fraction of the total number of connections, these few contributed to 15% and 61% of τ^2 for sheephead and kelpbass, respectively. This highlights that only a few regional connections are responsible for the drop in metapopulation growth rates when rare.

Clustering the weighted variance/covariance matrix (eq. [8]) revealed geographically distinct groups of subpopulation connections. In figure 3*c* and 3*d*, we show two pairs of groups for both our modeled kelp bass and sheephead species, which contribute to a large portion of τ^2 and the reduction in the metapopulation growth rate when rare. These groups are ordered on the basis of the number of connections in each group (first number in legend), and each connection is colored by its group rank τ_{xy}^2 value. The second number in the legend is $\sum_{\text{group}} \tau_{xy}^2$ normalized by τ^2. This value identifies the fractional contribution of a particular group to τ^2. Between species, these connection groups correspond to different geographically regions. Sheephead connections are groups around the islands in the south of the domain, whereas kelp bass connections are groups along the mainland. This highlights the large differences in the spatial and temporal properties of each species' potential connectivity, a result of the different pelagic larval durations and spawning periods (see the crosses in fig. 2*b*), and oceanographic currents they experience while dispersing. These connection groups also correspond to the geographic distribution of the top 1% of subpopulation connections (fig. 3*a*, 3*b*), indicating that these groups are important to the reduction in metapopulation growth rates when rare.

Temporal variability in potential connectivity also reduced metapopulation equilibrium abundances, with stationary distribution expectations lower by ~5%–40% (fig. 4; eq. [15]). Abundances were reduced most during the

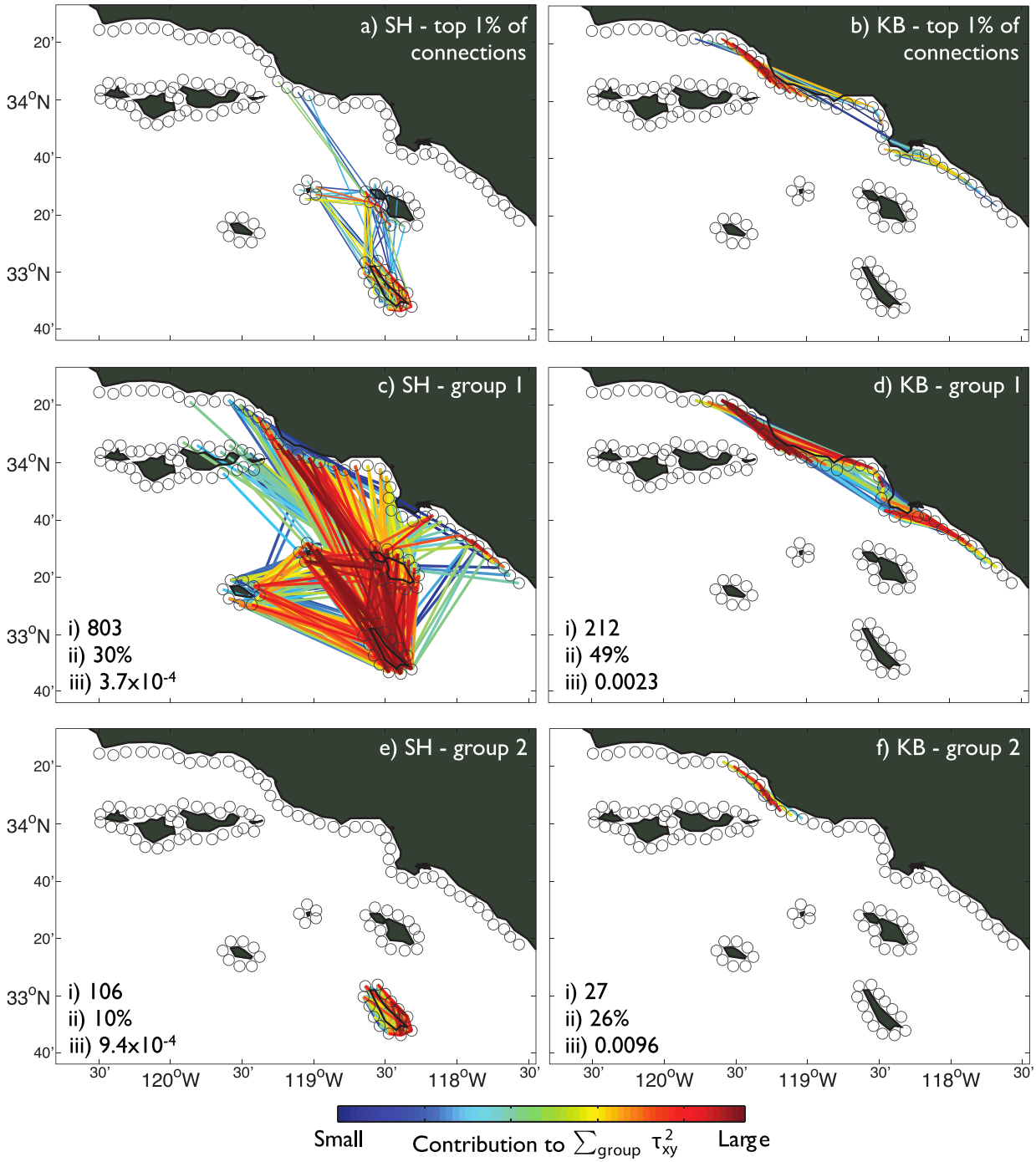

Figure 3: Top 1% of subpopulation connections (137 in total) contributing to τ^2, colored by their rank τ^2_{xy} value, for our simulated sheephead (*a*; 60-day pelagic larval duration [PLD], spring spawning) and kelp bass (*b*; 30-day PLD, fall spawning) species. We omit the exact τ^2 values and use the colors merely to identify the different connections. *c–f*, Groups of subpopulation connections derived from their weighted temporal covariances (eq. [8]) for sheephead (*c*, *e*; 60-day PLD, spring spawning) and kelp bass (*d–f*; 30-day PLD, fall spawning). Each connection is colored by its rank τ^2_{xy} value for its group; larger values are red, smaller values are blue. Panels are labeled by three numbers: (i) the number of edges in that group, (ii) the fractional contribution of a given groups' edges to τ^2 (i.e., $\sum_{\text{group}} \tau^2_{xy}$), and (iii) the average τ^2_{xy} value. Because $\sum_{\text{group}} \tau^2_{xy}$ values are positive, these groups reduce the metapopulation growth rate when rare.

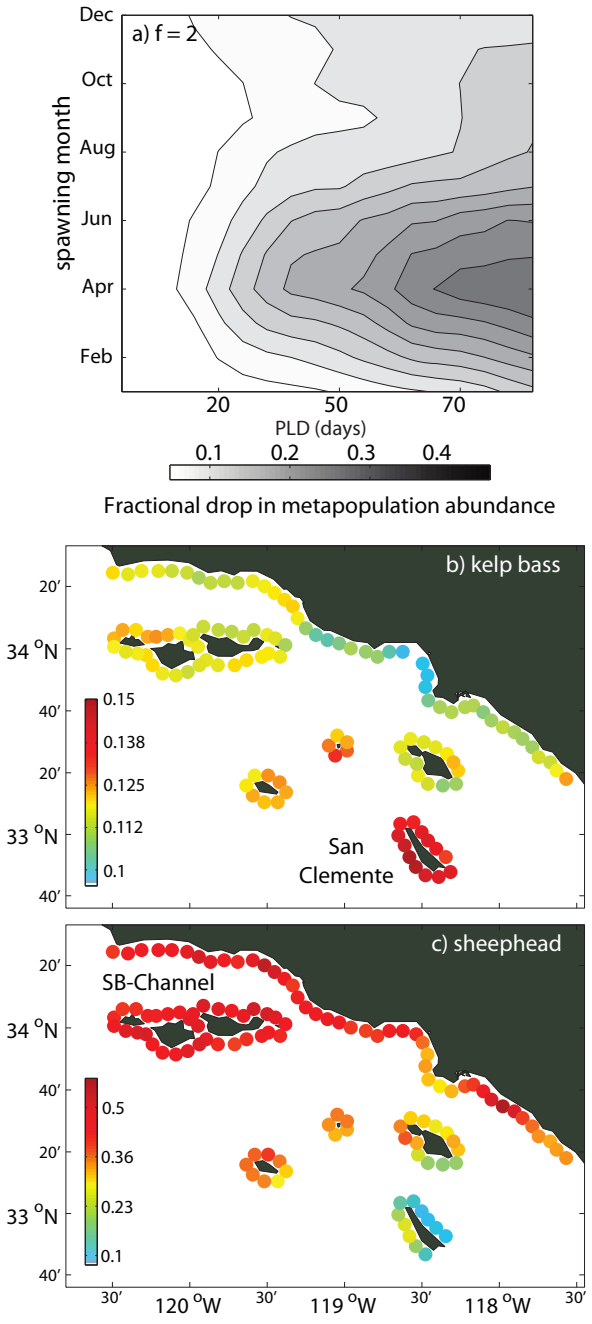

Figure 4: *a*, Fractional difference between the deterministic metapopulation equilibrium abundance and the stochastic stationary distribution expectation for fecundity = 2. Values are positive, indicating a drop in abundances. Values vary with pelagic larval duration (PLD; *X*-axis) and spawning period (*Y*-axis). *b*, *c*, Fractional drop in subpopulation equilibrium abundances that result from the stochasticity of potential connectivity for fecundity = 2 for our simulated kelp bass and sheephead species, respectively. Large values identify subpopulations that are most affected by stochastic potential connectivity. In general, sheephead subpopulation abundances reduce more than those of kelp bass, with the greatest change observed in the Santa Barbara Channel (SB-Channel). In contrast, kelp bass subpopulations on San Clemente island, in the south, drop the most.

spring spawning months (February–May) and at high pelagic larval durations (>50 days). This matches the spawning periods and pelagic larval durations that have the greatest variability in potential connectivity (fig. 2*a*). Species with low pelagic larval durations also have large variability in potential connectivity (fig. 2*a*), but they did not show large changes in equilibrium abundances. This indicates that for these species, even though there is variability in potential connectivity, there is little variability in the number of settlers at a given subpopulation. This occurs because at low pelagic larval durations, a given subpopulation receives settlers from numerous neighboring source subpopulations; hence, there is redundancy between connections. This redundancy mitigates the impact of temporal variability in potential connections.

The drop in equilibrium metapopulation abundances varied with the strength of density dependence, which was modulated by the fecundity parameter (see fig. A3, available online). We found that at higher fecundities (stronger density dependence), the difference between deterministic and stochastic outcomes was smaller than at lower fecundities (weaker density dependence). This is expected from analyzing equation (16); larger fecundities lead to higher levels of larval settlement ($E(s_x)$), which then reduces the impact of settlement variability, because $E(s_x)$ is in the denominator of the term in parentheses. Therefore, theoretically there exists a high level of density dependence (i.e., large f), where the difference between stochastic and deterministic outcomes is negligible. However, we chose fecundity values that created realistic levels of density dependence (values were taken from California Department of Fish and Game 2009; compensation ratios from 2.5 to 6), and this theoretical limit is likely far beyond what is actually experienced in nature (Bode et al. 2006).

Subpopulations responsible for the drop in metapopulation abundance were heterogeneously distributed throughout the Southern California Bight, with large differences between species (fig. 4*b*, 4*c*). Simulated kelp bass subpopulations showed greatest reductions in the south of the Southern California Bight (fig. 4*b*), whereas sheephead reductions were found mainly in the north of the domain (fig. 4*c*). Furthermore, sheephead subpopulations showed greater reductions in general (by a factor of 2 for $f = 2$). This again highlights the interspecific variability in nearshore species' potential connectivity and metapopulation dynamics.

The analytical approximation for the expected number

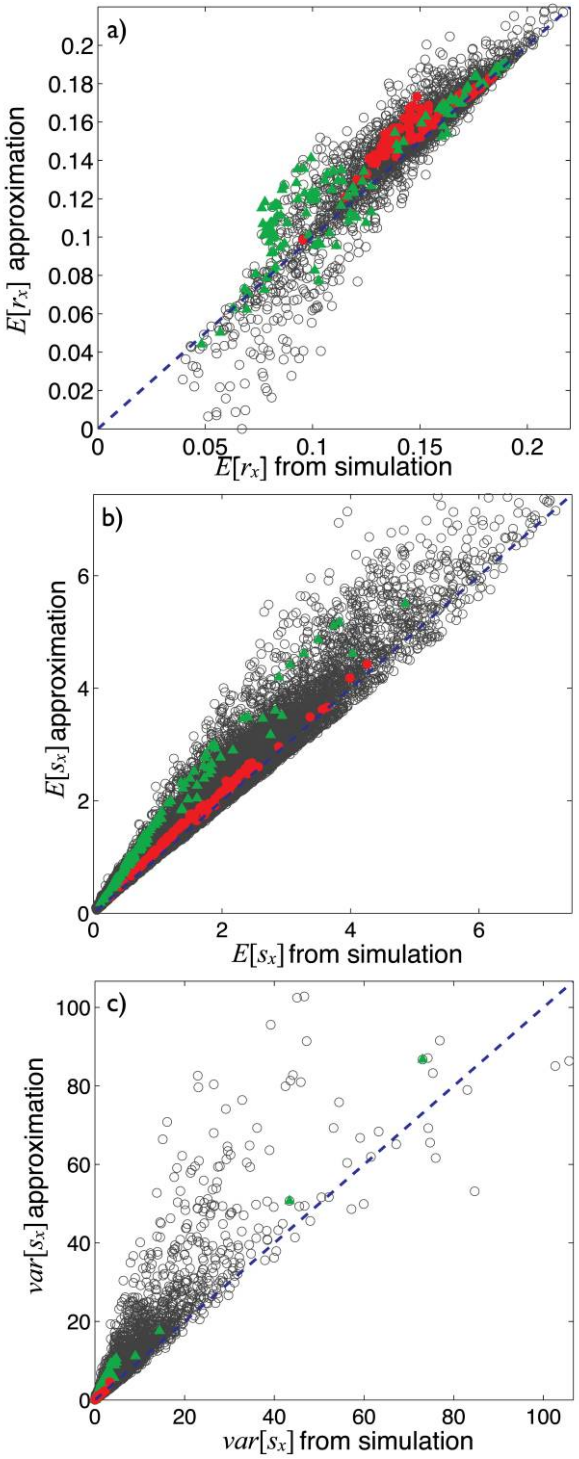

Figure 5: Relationships between various simulated and approximated metapopulation statistics at a medium level of density dependence (fecundity = 2; for the relationships under low and high levels of density dependence, see fig. A4, available online). *a*, Expected number of recruits (eq. [15]; linear regression $R^2 = 0.88$, slope = 0.87, intercept = 0.02). *b*, Expected number of settlers ($E(s_x)$; eq. [16]; linear regression $R^2 = 0.96$, slope = 1.07, intercept = 0.08). *c*, Variance in the number of settlers ($\mathrm{Var}(s_x)$; eq. [16]; linear regression $R^2 = 0.88$, slope = 1.28, intercept = 0.19). Gray circles identify the relationship for all species and all subpopulations, and red and green circles highlight the relationship for kelp bass and sheephead, respectively. The blue dashed line identifies the one-to-one line.

of recruits at a given subpopulation (eq. [15]) showed strong correspondence with simulation results (fig. 5*a*). This indicates that the variance in settlement is indeed responsible for the drop in equilibrium abundances. The further approximations for the expectation and variance in settlement, which assumed that adult abundances were constant through space and time (eq. [16]), also showed strong correspondence with simulated results (fig. 5*b*, 5*c*). These strong relationships confirm that it is the temporal variability in potential connectivity that drives the reductions in equilibrium adult abundances. The correlations within species (e.g., fig. 5, red and green circles) are stronger than when aggregated over all species (all gray circles). For the expectation and variance in settlement, the average within-species R^2 values were 0.99 and 0.98, respectively. Therefore, the spread is explained by the variation among species in the slope of the relationship. These relationships were maintained as the strength of density dependence was varied (see fig. A4, available online).

The further approximations for the expectation and variance in settlement showed a bias to larger values. The bias indicates that the covariances between adult abundances and potential connections, which were ignored in the further approximation, are negative. Further, the settlement distributions through time were highly nonnormal, and hence the truncation of higher moments in the Taylor expansion contributed to the bias. However, because the overall relationships are so strong, the bias does not invalidate the result: the temporal variability of potential connectivity is the principal factor creating differences between deterministic and stochastic outcomes.

Discussion

Through analyzing a simple metapopulation model, we showed that temporal variability in potential connectivity alters both metapopulation growth rates when a species is rare and equilibrium abundances. We further showed that for a specific case—nearshore marine species in the Southern California Bight—these changes are negative, with decreases in both demographic quantities. Relative to deterministic outcomes, where connectivity is constant through

time, metapopulation growth rates when rare dropped by ~10%–30% and equilibrium abundances dropped by ~5%–40%, depending on the species. Metapopulation dynamics when rare and when abundant were both well described by the Tuljapurkar (eqq. [7], [8]) and Taylor expansion (eq. [15]) approximations, respectively. These approximations revealed that it is covariances between connections that drive changes in growth rates when rare and that the variability in larval settlement drives changes in equilibrium abundances. These changes are not small, indicating that this form of environmental stochasticity strongly influences nearshore metapopulation dynamics, and as a result, it is an important consideration for anyone seeking to understand and quantify the demographics of nearshore marine species.

The Southern California Bight can also be divided into geographically distinct regions on the basis of the subpopulation connection covariances and sensitivities of particular species (i.e., the weighted covariance matrix in Tuljapurkar's approximation; eqq. [7], [8]; fig. 3*c*–3*f*). These regions varied in size and contribution to the reduction in growth rates when rare and varied greatly between species. This is a novel source of spatially explicit information for fisheries managers and conservation scientists. For example, these regions identify areas that would contribute differentially to the recovery of an overexploited stock. One could go further and analyze the components of Tuljapurkar's approximation and, for example, identify regions with synchronized connections. Synchrony in metapopulations has been studied extensively because it has a strong effect on persistence. However, most attention has been paid to the synchronizing effect of temporally correlated disturbances (e.g., Day and Possingham 1995; Johst and Drechsler 2003; Elkin and Possingham 2008). Our results show that in nearshore systems, there is another force promoting population synchrony: the seascape itself, through the effect of ocean circulation on potential connectivity.

These results highlight the influence of potential connectivity's temporal variability on metapopulation dynamics. Yet, this form of environmental stochasticity is rarely included in fisheries or conservation analyses (Bousquet et al. 2008; Aiken and Navarrete 2011). For example, surplus production models are a traditional first analytical tool for stock assessment (Jensen 2002). A key quantity typically addressed by these models is the maximum sustainable yield, which is defined as the maximal possible catch such that the population biomass can continue to regenerate (Hilborn and Walters 1992). The maximum sustainable yield remains a key parameter in many stock assessment and harvest strategy models, and yet it is typically found using deterministic calculations (Bousquet et al. 2008). Stochastic potential connectivity is exactly the type of time-varying process that will affect determinations of maximum sustainable yield and any management strategy derived from it. Given the large changes in metapopulation growth rates when rare and equilibrium abundances, incorporating this source of stochasticity into surplus production models will be a key step to generating more accurate fisheries management plans.

Protected areas are a popular tool for conservation and management on land and in the sea (Possingham et al. 2000; Lubchenco et al. 2003; Roberts et al. 2003; Botsford et al. 2009; California Department of Fish and Game 2009). Metapopulation analyses contribute to the design of protected areas by identifying critical habitat patches. For example, there are many methods for identifying the location of hub subpopulations, those that act as migratory focal points (Ovaskainen and Hanski 2003; Bodin and Saura 2010; Jacobi and Jonsson 2011; Watson et al. 2011*b*), or source subpopulations, those that produce the most new recruits (Bode et al. 2006). These critical subpopulations contribute to metapopulation persistence and are ideal candidates for protection from disturbance (Ovaskainen and Hanski 2003). What, then, does it mean that a subpopulation is a good source or hub one year but not the next? We do not attempt to answer this question here, but the theory borrowed from stage-structured modeling again lends insight. In these models, the stochastic reproductive value (Caswell 2001) identifies the contribution of each stage to the stochastic growth rate of the stage-structured population (i.e., λ_s). In our setting, this metric would quantify the contribution of a given subpopulation to the stochastic metapopulation growth rate, precisely what is needed to identify critical regions for protection in a stochastic world.

Stochastic potential connectivity can also be used to inform management by identifying critical connections. In our analysis of the Southern California Bight, we quantified deterministic sensitivities (eq. [8]; $\partial\lambda_1/\partial C_{xy}$) and the contribution of each subpopulation connection to the difference in deterministic and stochastic growth rates when rare (eq. [8]; τ^2_{xy}). Going further, one could calculate stochastic sensitivities (i.e., $\partial\lambda_s$ with respect to either the mean or the variance of C_{xy}; Tuljapurkar et al. 2003), which identify those connections that are most important to the stochastic metapopulation growth rate when rare (λ_s; Caswell 2001). Protecting these critical connections is another way to secure metapopulation growth rates when rare and offers an important management alternative to protecting critical subpopulations (Hastings and Botsford 2006).

Temporal variability in connectivity is not the only source of environmental stochasticity for natural systems (Lande and Orzack 1988; Aiken and Navarrete 2011; Gravel et al. 2011; Shelton and Mangel 2011). Another is the amount of suitable habitat. For example, in the South-

ern California Bight, kelp forests are the primary habitat for nearshore marine species (Steneck et al. 2002; Graham et al. 2007), with kelp forest size linked to larval production and the strength of postsettlement density dependence (White and Caselle 2008). Kelp forests are known to be ephemeral, varying seasonally with winter storms and summer regrowth. For example, Cavanaugh et al. (2011) showed that at regional scales (~100 km) in the Southern California Bight, giant kelp biomass has a temporal coefficient of variation ~1, yet in our analysis, we assumed that suitable habitat was constant through time and uniformly distributed. Assessing the impact of this additional source of environmental stochasticity will be another important step toward making more accurate determinations of the population dynamics of nearshore marine species. Marine systems are known to have large fluctuations in the recruitment of new individuals (Shelton and Mangel 2011), and it remains a challenge to identify the most influential forces causing populations to fluctuate in abundance.

A limitation to our numerical approach is the short 7-year connectivity time series we used. This is not enough to capture decadal periodicities in the Southern California Bight's circulation, for example, those that result from the Pacific Decadal Oscillation or the North Pacific Gyre Oscillation (Di Lorenzo et al. 2008). These oceanographic features may produce time-varying deterministic dynamics, in contrast to the purely time-varying stochastic dynamics we have addressed here. Indeed, periodic forcing in marine environments may demand a whole different class of analyses (e.g., Floquet theory; Klausmeier 2008). Another limitation is that we assumed that larvae are unable to alter their own dispersal and that passive Lagrangian particles simulate their dispersal. Considerable evidence suggests that larval behavior, such as vertical mobility or late-stage homing, can significantly alter the spatial patterns of connectivity (Leis 2007; Pfeiffer-Herbert et al. 2007). However, while the details of the spatial patterns of potential connectivity might be affected by behavior, the relative importance of stochasticity probably will not. Potential connectivity will vary in time, and deterministic analyses that ignore this source of environmental stochasticity will overestimate growth rates and abundances.

Regardless of these potential limitations, our general conclusion holds: for certain nearshore marine species, the temporal variance and covariances in dispersal probabilities can be just as important as the spatial patterns they describe. Hence, using time-averaged data or indeed data from just 1 year's worth of simulation, which is common, is ill advised. This reasoning is not just applicable to the nearshore for there are a number of other systems where potential connectivity may have large temporal variability, for example, riverine (e.g., Muneepeerakul et al. 2008), wind-dispersed (e.g., Drake and Farrow 1989), and socioecological systems (e.g., Bossenbroek et al. 2001). Similar to nearshore metapopulations, modeling results for these systems will likely be inaccurate if potential connectivity is assumed constant.

Acknowledgments

We thank C. Dong and J. McWilliams for sharing the regional ocean modeling system model solutions, the members of the Flow Fish Fishing National Science Foundation (NSF) Biocomplexity project (especially H. Berkley, A. Rassweiler, and C. White), J. Elliott, and two anonymous reviewers for their help in preparing this article. Funding was provided by the National Aeronautics and Space Administration and the NSF.

Literature Cited

Aiken, C., and S. Navarrete. 2011. Environmental fluctuations and asymmetrical dispersal: generalized stability theory for studying metapopulation persistence and marine protected areas. Marine Ecology Progress Series 428:77–88, doi:10.3354/meps09079.

Berkley, H., B. Kendall, S. Mitarai, and D. Siegel. 2010. Turbulent dispersal promotes species coexistence. Ecology Letters 13:360–371.

Blackwood, J., A. Hastings, and C. Costello. 2010. Cost-effective management of invasive species using linear-quadratic control. Ecological Economics 69:519–527.

Bode, M., L. Bode, and P. R. Armsworth. 2006. Larval dispersal reveals regional sources and sinks in the Great Barrier Reef. Marine Ecology Progress Series 308:17–25.

Bodin, O., and S. Saura. 2010. Ranking individual habitat patches as connectivity providers: integrating network analysis and patch removal experiments. Ecological Modelling 221:2393–2405.

Bossenbroek, J., C. Kraft, and J. C. Nekola. 2001. Prediction of long-distance dispersal using gravity models: zebra mussel invasion of inland lakes. Ecological Applications 11:1778–1788.

Botsford, L., D. Brumbaugh, C. Grimes, J. Kellner, J. Largier, M. O. Farrell, S. Ralston, E. Soulanille, and V. Wespestad. 2009. Connectivity, sustainability, and yield: bridging the gap between conventional fisheries management and marine protected areas. Reviews in Fish Biology and Fisheries 19:69–95.

Botsford, L., F. Micheli, and A. Hastings. 2003. Principles for the design of marine reserves. Ecological Applications 13:25–31.

Bousquet, N., T. Duchesne, and L. Rivest. 2008. Redefining the maximum sustainable yield for the Schaefer population model including multiplicative environmental noise. Journal of Theoretical Biology 254:65–75, doi:10.1016/j.jtbi.2008.04.025.

California Department of Fish and Game. 2009. California Marine Life Protection Act. http://www.dfg.ca.gov/mlpa/.

Caswell, H. 2001. Matrix population models: construction, analysis, and interpretation. Sinauer, Sunderland, MA.

Cavanaugh, K. C., D. A. Siegel, D. C. Reed, and P. E. Dennison. 2011. Environmental controls of giant-kelp biomass in the Santa

Barbara Channel, California. Marine Ecology Progress Series 429: 1–17.

Cowen, R., C. Paris, and A. Srinivasan. 2006. Scaling of connectivity in marine populations. Science 311:522–527.

Day, J., and H. Possingham. 1995. A stochastic metapopulation model with variability in patch size and position. Theoretical Population Biology 48:333–360.

Di Lorenzo, E., N. Schneider, K. M. Cobb, P. J. S. Franks, K. Chhak, A. J. Miller, J. C. McWilliams, et al. 2008. North Pacific Gyre Oscillation links ocean climate and ecosystem change. Geophysical Research Letters 35:L08607.

Dong, C., E. Idica, and J. McWilliams. 2009. Circulation and multiple-scale variability in the Southern California Bight. Progress in Oceanography 82:168–190.

Drake, V. A., and R. A. Farrow. 1989. The aerial plankton and atmospheric convergence. Trends in Ecology & Evolution 4:381–385, doi:10.1016/0169-5347(89)90107-9.

Elkin, C. M., and H. Possingham. 2008. The role of landscape-dependent disturbance and dispersal in metapopulation persistence. American Naturalist 172:563–575, doi:10.1086/590962.

Goodyear, C. 1980. Compensation in fish populations. Pages 253–280 *in* C. H. Hocutt and J. R. Stauffer, eds. Biological monitoring of fish. Lexington Books, Lexington.

Graham, M., J. Vasquez, and A. Buschmann. 2007. Global ecology of the giant kelp *Macrocystis*: from ecotypes to ecosystems. Oceanography and Marine Biology Annual Review 45:39–88.

Gravel, D., F. Guichard, and M. E. Hochberg. 2011. Species coexistence in a variable world. Ecology Letters 14:828–839, doi: 10.1111/j.1461-0248.2011.01643.x.

Hanski, I. 1998. Metapopulation dynamics. Nature 396:41–50.

Hastings, A., and L. Botsford. 2006. Persistence of spatial populations depends on returning home. Proceedings of the National Academy of Sciences of the USA 103:6067–6072.

Hilborn, R., and C. Walters. 1992. Quantitative fisheries stock assessment: choice, dynamics and uncertainty. Book, New York.

Jacobi, M. N., and P. R. Jonsson. 2011. Optimal networks of nature reserves can be found through eigenvalue perturbation theory of the connectivity matrix. Ecological Applications 21:1861–1870.

Jensen, A. L. 2002. Maximum harvest of a fish population that has the smallest impact on population biomass. Fisheries Research 57: 89–91, doi:10.1016/S0165-7836(01)00337-X.

Johst, K., and M. Drechsler. 2003. Are spatially correlated or uncorrelated disturbance regimes better for the survival of species? Oikos 103:449–456.

Kinlan, B., S. Gaines, and S. Lester. 2005. Propagule dispersal and the scales of marine community process. Diversity and Distributions 11:139–148.

Klausmeier, C. A. 2008. Floquet theory: a useful tool for understanding nonequilibrium dynamics. Theoretical Ecology 1:153–161, doi: 10.1007/s12080-008-0016-2.

Lande, R., and S. H. Orzack. 1988. Extinction dynamics of age-structured populations in a fluctuating environment. Proceedings of the National Academy of Sciences of the USA 85:7418–7421.

Largier, J. 2003. Considerations in estimating larval dispersal distances from oceanographic data. Ecological Applications 13:S71–S89.

Leis, J. 2007. Behaviour as input for modelling dispersal of fish larvae: behaviour, biogeography, hydrodynamics, ontogeny, physiology and phylogeny meet hydrography. Marine Ecological Progress Series 347:185–193.

Love, M. S. 1991. Probably more than you want to know about the fishes of the Pacific Coast. Really Big, Santa Barbara, CA.

Lubchenco, J., S. Palumbi, S. D. Gaines, and S. Andelman. 2003. Plugging a hole in the ocean: the emerging science of marine reserves. Ecological Applications 13:S3–S7.

McRae, B., B. Dickson, T. Keitt, and V. Shah. 2008. Using circuit theory to model connectivity in ecology, evolution, and conservation. Ecology 89:2712–2724.

Mitarai, S., D. Siegel, J. Watson, C. Dong, and J. C. McWilliams. 2009. Quantifying connectivity in the coastal ocean with application to the Southern California Bight. Journal of Geophysical Research 114:C10026, doi:10.1029/2008JC005166.

Morris, W. F., and D. F. Doak. 2002. Quantitative conservation biology: theory and practice of population viability analysis. Sinauer, Sunderland, MA.

Muneepeerakul, R., E. Bertuzzo, H. J. Lynch, W. F. Fagan, A. Rinaldo, and I. Rodriguez-Iturbe. 2008. Neutral metacommunity models predict fish diversity patterns in Mississippi-Missouri basin. Nature 453:220–222, doi:10.1038/nature06813.

Ohlmann, J. C., and S. Mitarai. 2010. Lagrangian assessment of simulated surface current dispersion in the coastal ocean. Geophysical Research Letters 37:L17602, doi:10.1029/2010GL044436.

Okubo, A., and S. A. Levin. 1989. A theoretical framework for data analysis of wind dispersal of seeds and pollen. Ecology 70:329–338, doi:10.2307/1937537.

Ovaskainen, O., and I. Hanski. 2003. How much does an individual habitat fragment contribute to metapopulation dynamics and persistence? Theoretical Population Biology 64:481–495.

Pfeiffer-Herbert, A. S., M. A. McManus, P. T. Raimondi, Y. Chao, and F. Chai. 2007. Dispersal of barnacle larvae along the central California coast: a modeling study. Limnology and Oceanography 52:1559–1569.

Possingham, H., I. Ball, and S. Andelman. 2000. Mathematical methods for identifying representative reserve networks. Pages 291–305 *in* S. Ferson and M. Burgman, eds. Quantitative methods for conservation biology. Springer, New York.

Roberts, C., S. Andelman, G. Branch, R. H. Bustamante, J. C. Castilla, J. Dugan, B. S. Halpern, et al. 2003. Ecological criteria for evaluating candidate sites for marine reserves. Ecological Applications 13:S199–S214.

Roughgarden, J., S. Gaines, and H. Possingham. 1988. Recruitment dynamics in complex life cycles. Science 241:1460–1466.

Ruel, J. J., and M. P. Ayres. 1999. Jensen's inequality predicts effects of environmental variation. Trends in Ecology & Evolution 14: 361–366.

Shelton, A. O., and M. Mangel. 2011. Fluctuations of fish populations and the magnifying effects of fishing. Proceedings of the National Academy of Sciences of the USA 108:7075–7080.

Siegel, D. A., S. Mitarai, C. J. Costello, S. D. Gaines, B. E. Kendall, R. R. Warner, and K. B. Winters. 2008. The stochastic nature of larval connectivity among nearshore marine populations. Proceedings of the National Academy of Sciences of the USA 105: 8974–8979.

Steneck, R. S., M. H. Graham, B. J. Bourque, D. Corbett, J. M. Erlandson, J. A. Estes, and M. J. Tegner. 2002. Kelp forest ecosystems: biodiversity, stability, resilience and future. Environmental Conservation 29:436–459.

Tilman, D., and P. Kareiva. 1997. Spatial ecology: the role of space in population dynamics and interspecific interactions. Princeton University Press, Princeton, NJ.

Treml, E. A., P. N. Halpin, D. L. Urban, and L. F. Pratson. 2008. Modeling population connectivity by ocean currents, a graph-theoretic approach for marine conservation. Landscape Ecology 23:19–36.

Tuljapurkar, S., C. Horvitz, and J. Pascarella. 2003. The many growth rates and elasticities of populations in random environments. American Naturalist 162:489–502.

Tuljapurkar, S., and S. Orzack. 1980. Population dynamics in variable environments. I. Long-run growth rates and extinction. Theoretical Population Biology 18:314–342.

Urban, D., E. Minor, E. Treml, and R. Schick. 2009. Graph models of habitat mosaics. Ecology Letters 12:260–273.

Vance, R. 1973. On reproductive strategies in marine benthic invertebrates. American Naturalist 107:339–352.

Watson, J. R., C. Hays, P. Raimondi, S. Mitarai, C. Dong, J. C. McWilliams, C. A. Blanchette, J. E. Caselle, D. A. Siegel. 2011*a*. Currents connecting communities: nearshore community similarity and ocean circulation. Ecology 92:1193–1200.

Watson, J. R., S. Mitarai, D. Siegel, J. Caselle, C. Dong, and J. C. McWilliams. 2010. Realized and potential larval connectivity in the Southern California Bight. Marine Ecology Progress Series 401: 31–48.

Watson, J. R., D. A. Siegel, B. E. Kendall, S. Mitarai, A. Rassweiller, and S. Gaines. 2011*b*. Identifying critical regions in small-world marine metapopulations. Proceedings of the National Academy of Sciences of the USA 108:E907–E913.

White, J., and J. Caselle. 2008. Scale-dependent changes in the importance of larval supply and habitat to abundance of a reef fish. Ecology 89:1323–1333.

With, K. 2002. The landscape ecology of invasive spread. Conservation Biology 16:1192–1203.

Associate Editor: Benjamin M. Bolker
Editor: Ruth G. Shaw

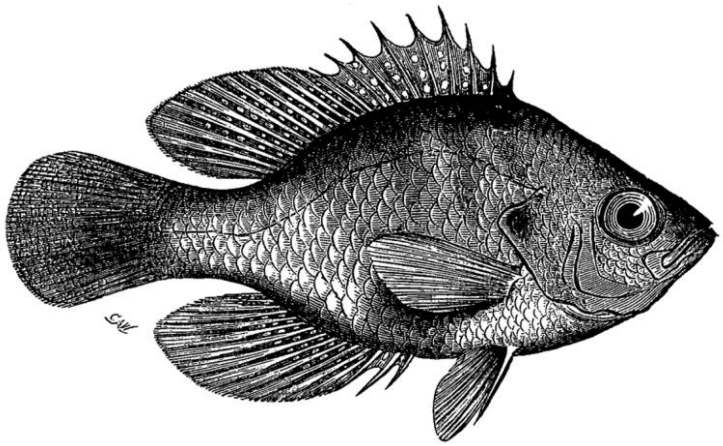

Spotted sunfish *Enneacanthus guttatus*. "So purely a mud-dwelling fish are they that we have frequently found them in water so shallow, that they marked the mud with their pectoral fins in swimming, preferring such shallow water, with mud, to that which was deeper, to which they had access, because it was over a stony bed." From "Mud-Loving Fishes" by Charles C. Abbott (*American Naturalist*, 1870, 4: 385–391).